EPJ Web of Conferences **106**, 06003 (2016)
DOI: 10.1051/epjconf/201610606003

The ^{235}U Prompt Fission Neutron Spectrum in the BR1 Reactor at SCK•CEN

Jan Wagemans[a], Edouard Malambu, Luc Borms, and Luca Fiorito

SCK•CEN, Boeretang 200, 2400 Mol, Belgium

Abstract. The BR1 research reactor at SCK•CEN has a spherical cavity in the graphite above the reactor core. In this cavity an accurately characterised Maxwellian thermal neutron field is present. Different converters can be loaded in the cavity in order to obtain other types of neutron (and gamma) irradiation fields. Inside the so-called MARK III converter a fast ^{235}U(n,f) prompt fission neutron field can be obtained. With the support of MCNP calculations, irradiations in MARK III can be directly related to the pure ^{235}U(n,f) prompt fission neutron spectrum. For this purpose MARK III spectrum averaged cross sections for the most relevant fluence dosimetry reactions have been determined. A calibration factor for absolute measurements has been determined applying activation dosimetry following ISO/IEC 17025 standards.

1. Introduction

The availability of standard irradiation fields is of primary importance for several applications including reactor dosimetry. Nowadays however only a few of such facilities are operational. Reference [1] presents an overview of the existing reference thermal neutron fields. Fast neutron irradiation fields can be obtained for example from radionuclide sources like ^{252}Cf. In addition to such nearly unperturbed irradiation fieds, ^{235}U Prompt Fission Neutron Spectrum (PFNS) irradiation fields are of particular interest as neutron induced fission on ^{235}U is the main neutron source in the present nuclear reactors.

The BR1 reactor at SCK•CEN provides various standard irradiation fields that have been recently revisited. An overview of the different irradiation fields and the preliminary results of its qualification are presented in [2]. The current paper presents the results of the characterisation of the so-called MARK III ^{235}U PFNS irradiation field.

First a brief overview of the BR1 reactor and its irradiation possibilities is presented. The main part of this paper is devoted to the ^{235}U PFNS in MARK III. After a short description of the MARK III device, it is explained how the spectrum averaged cross sections for the main fluence dosimetry reactions have been calculated. Then the experimental validation is presented, and finally it is explained

[a] Corresponding author: jwageman@sckcen.be

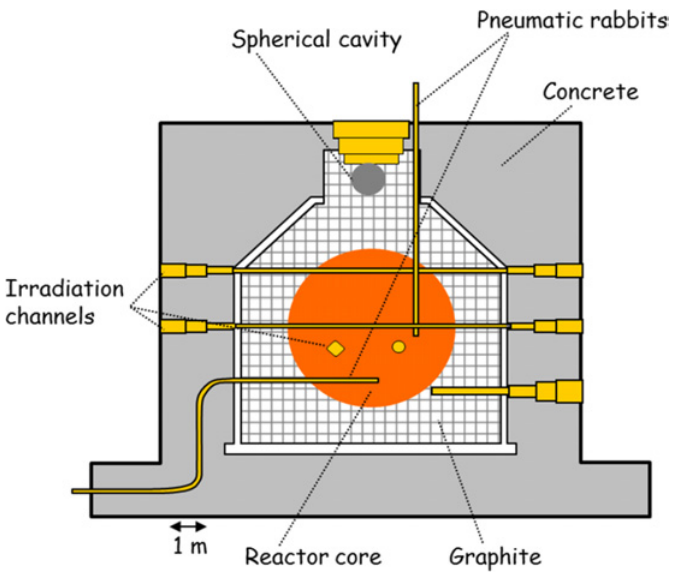

Figure 1. Schematic drawing of the BR1 reactor.

how a calibration factor and corrections for neutron flux gradients have to be applied for calibration measurements inside MARK III. The paper concludes with some nuclear data considerations that "appeared" during this work.

2. The BR1 Reactor

The BR1 reactor is a research reactor that uses natural metallic uranium as fuel, graphite as moderator and circulation of air for the cooling. It is operated on a daily basis at a maximum power of 700 kW or at 1 MW for short time periods of a few hours.

The reactor consists of a matrix of a graphite volume of $6.7 \times 6.7 \times 6.8\,\mathrm{m}^3$. In this volume 829 fuel channels are foreseen, of which 552 are loaded with fuel in the current configuration. The core loading is approximately cylindrical with a diameter of 4.7 m and a length of 4.9 m. Each fuel channel contains 23 fuel rods of 21.4 cm lenght, consisting of natural metallic uranium in an aluminium cladding.

About 50 irradiation channels penetrate the reactor core, either parallel or perpendicular to the fuel. These irradiation channels can be used for in-core and ex-core experiments. The maximum thermal neutron flux in the centre of the core is about $5\times10^{11}\,\mathrm{cm}^{-2}\,\mathrm{s}^{-1}$. Thanks to the large reactor core volume, the neutron flux gradients are low (about 10% per meter around the core centre). At one of the irradiation channels a neutrography device is installed. The BR1 reactor is also equipped with a pneumatic rabbit system allowing injection of samples into different positions in the reactor core.

A schematic view of the BR1 reactor is shown in Fig. 1. The graphite (hatched region) is extended vertically to constitute a thermal column above the reactor core. Here a spherical cavity of 1 m diameter is machined in the graphite. The fast neutrons coming from the fission reactions in the reactor core are completely thermalised before entering the cavity. Therefore the neutron flux inside the cavity follows a Maxwellian distribution at room temperature. At a reactor power of 1 MW the thermal neutron flux in the centre of the cavity is $1.0 \times 10^9\,\mathrm{cm}^{-2}\,\mathrm{s}^{-1}$.

The thermal neutrons inside the cavity can be used as a driver of other types of irradiation fields by loading specific converters in the cavity. Three different types are available:

- Spherical shells made of Fe, Cu and U to obtain mixed neutron-gamma fields;
- Cylindrical converters containing so-called black absorber foils (Cd, B, Co) to obtain prompt capture gamma fields.
- Cylindrical converters with a high-enriched uranium foil mounted on a Cd tube to obtain a ^{235}U PFNS field. MARK III is the most important of these and its characteristics will be the subject of the remaining part of this paper.

The normalisation of the experiments performed in the cavity is achieved using a calibration factor that is constant for all reactor powers ranging from 10^2 to 10^6 W. The calibration factor is the ratio of the neutron flux in the centre of the cavity to the monitor fission chamber count rate. The neutron flux is derived from neutron activation dosimetry measurements in the centre of the cavity. The monitor fission chamber is a fission chamber that is located outside and close to the cavity. The count rate of this monitor fission chamber is continuously logged and is independent of any device or experiment that is loaded in the cavity.

In order to complement the experimental characterisation of the irradiation fields in BR1, a fully detailed model of the reactor has been developed for neutron transport simulations with MCNP Monte Carlo codes. In this way accurate knowledge of the neutron spectra in the various irradiation positions can be obtained. Moreover this tool can be used to determine problem–dependent correction factors for detector calibrations and irradiation experiments.

3. The ^{235}U Prompt Fission Neutron Spectrum in the MARK III Converter

3.1 The MARK III Converter

The MARK III converter consists of a 2 m long cadmium tube, with an inner diameter of 48 mm and a thickness of 1 mm. It can be loaded in the cavity of the BR1 reactor from the top of the reactor. The bottom of the tube is closed with a cadmium plate while the top is open just above the reactor shielding to allow easy access for experiments. The fission source is a 90 wt.% enriched ^{235}U foil of 8 cm length and 0.38 mm thickness in an aluminium cladding mounted on (outside) the cadmium tube. The MARK III converter is loaded in the cavity such that the fission source is positioned in the centre of the cavity. A cylindrical aluminium tube of about 2 m length is used to accurately position samples in the MARK III.

A schematic drawing of the MARK III converter loaded in the cavity is presented in Fig. 2. The position of the monitor fission chamber is also shown.

3.2 Calculated Neutron Spectrum in MARK III and Experimental Validation

The neutron spectrum in the MARK III device slightly deviates from the “pure” ^{235}U(n,f) PFNS due to the presence of structural materials. Therefore correction factors are required for irradiations that need to be directly referred to the ^{235}U(n,f) PFNS.

Therefore a full 3-D geometrical model of the BR1 reactor was made for the Monte-Carlo simulations. These were carried out using the MCNP5-1.60 code version [3], running in a parallel computer environment with MPI-multiprocessing, along with continuous pointwise cross-sections from the ENDF/B-VII.1 nuclear data [4]. Due to the geometry complexity and size, it turned out to be almost impossible to achieve good statistics on neutron spectra and reaction rates inside the MARK III device. Therefore a two-step calculation scheme using the Surface Source Write – Surface Source Read capabilities of the MCNP code was adopted. The first step consists of running a criticality calculation using the full BR1 core model to create a surface neutron source file which records the tracks of the

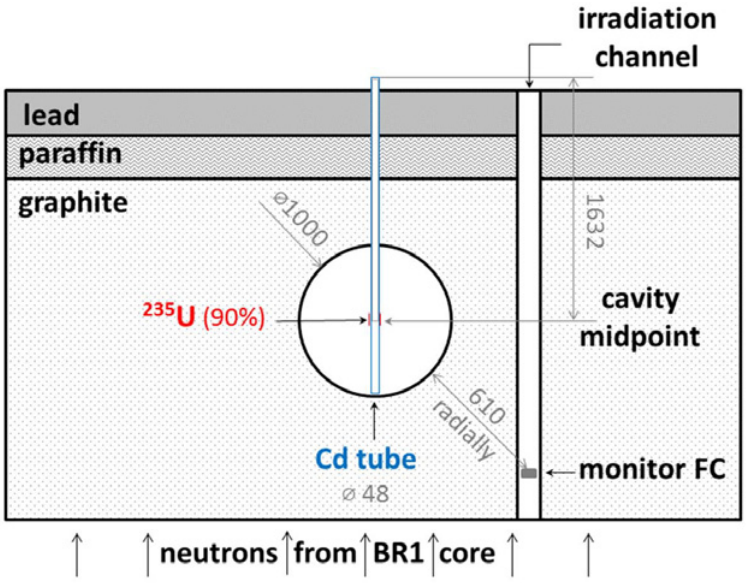

Figure 2. Schematic drawing of the MARK III in the cavity and the monitor fission chamber. Dimensions are in mm.

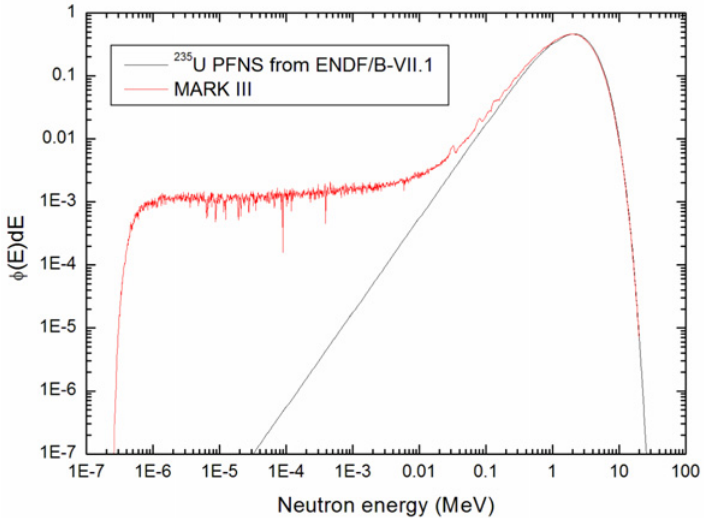

Figure 3. MARK III spectrum calculated with MCNP and ^{235}U PFNS from ENDF/B-VII.1.

individual neutrons crossing a spherical surface of 65 cm radius (concentric with the cavity) streaming towards the cavity. This source file is for a subsequent local calculation where the geometry model is limited to the vertical column. MCNP enables to increase the number of the source particules thereby improving the statistics of the tallies in the local calculation.

Figure 3 shows the neutron spectrum obtained with MCNP calculations in the centre of the MARK III converter. The ^{235}U PFNS from ENDF/B-VII.1 used in the MCNP simulations is also plotted. This ^{235}U PFNS is a pointwise curve obtained from the Los Alamos fission Maddland-Nix model.

Table 1. Activation threshold reactions used in the MARK III spectrum with corresponding response ranges and calibration factors.

reaction	E_{50}(MeV)	calibration factor	uncertainty (%)
^{115}In(n,n′)	2.1	8879	3.4
^{58}Ni(n,p)	3.6	8722	2.7
^{54}Fe(n,p)	4.7	8578	3.3
^{27}Al(n,p)	5.2	8818	3.3
^{56}Fe(n,p)	6.9	8616	3.5
^{27}Al(n,α)	8.0	8552	2.3

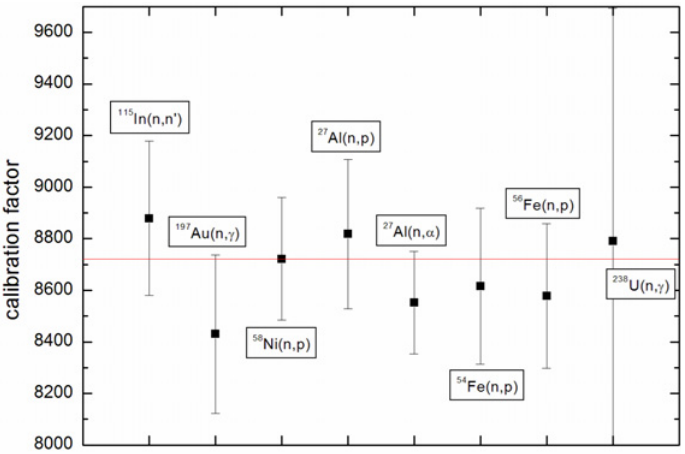

Figure 4. Calibration factors obtained with different dosimeters. The red line represents the value obtained from the ^{58}Ni(n,p) reaction.

The epithermal part in the MARK III neutron spectrum is mainly due to backscattering in the surrounding graphite.

An experimental validation of the MARK III spectrum was performed via activation dosimetry. For that purpose, a set of dosimeters was selected in such a way that a broad energy range was covered by the reaction responses, and that allow accurate activity measurements. For each reaction the calibration factor was determined combining the measured reaction rate ($\sim$ activity), the MARK III spectrum averaged cross section (see further) and the monitor fission chamber count rate. The results are shown in Table 1 and Fig. 4. The E_50 response range (half of the detector response occurs below the energy E_{50}) of the threshold reactions in the MARK III spectrum is also presented in Table 1. The 1σ uncertainties include the experimental uncertainty and the uncertainty on the calculated cross section (obtained from the covariance data). All reactions are compared to the ^{58}Ni(n,p) reaction. One observes that the calibration factors obtained with all the reactions (including ^{238}U(n,γ) and ^{197}Au(n,γ) with thermal-epithermal response) agree within the uncertainties. The entire experimental validation has been performed following approved ISO/IEC 17025 standards.

3.3 Calibrations in Mark 3

In order to perform calibrations in an irradiation field like MARK III, neutron spectrum averaged cross sections and neutron flux have to be known. This is detailed below.

Table 2. MARK III spectrum averaged cross sections.

reaction	cross section (mb)	uncertainty (%)	library*
^{24}Mg(n,p)	1.35	0.83	IRDFF-1.02
^{27}Al(n,p)	3.56	2.06	IRDFF-1.02
^{27}Al(n,α)	0.64	0.74	IRDFF-1.02
^{46}Ti(n,p)	10.3	3.19	IRDFF-1.02
^{47}Ti(n,p)	16.6	2.78	IRDFF-1.02
^{48}Ti(n,p)	0.27	5.59	IRDFF-1.02
^{54}Fe(n,p)	72.7	2.12	IRDFF-1.02
^{54}Fe(n,α)	0.76	3.97	IRDFF-1.02
^{56}Fe(n,p)	0.98	2.69	IRDFF-1.02
^{58}Ni(n,p)	97.5	1.75	IRDFF-1.02
^{115}In(n,γ)	3058	5.73	IRDFF-1.02
^{115}In(n,n$'$)	173.9	1.68	IRDFF-1.02
^{197}Au(n,γ)	1792	1.99	IRDFF-1.02
^{232}Th(n,f)	69.9	2.11	IRDFF-1.02
^{234}U(n,f)	1133	19.3	JEFF-3.1.2
^{235}U(n,f)	1494	0.23	IRDFF-1.02
^{236}U(n,f)	571.8	24.4	JEFF-3.1.2
^{238}U(n,f)	285.7	0.52	IRDFF-1.02
^{238}U(n,γ)	273.5	1.94	IRDFF-1.02
^{237}Np(n,f)	1290	1.68	IRDFF-1.02
^{238}Pu(n,f)	1972	0.68	JEFF-3.1.2
^{239}Pu(n,f)	2131	0.43	IRDFF-1.02
^{240}Pu(n,f)	1308	0.52	JEFF-3.1.2
^{242}Pu(n,f)	1116	1.87	JEFF-3.1.2
^{241}Am(n,f)	1314	2.75	IRDFF-1.02
^{242}Am(n,f)	1024	0.98	JEFF-3.1.2

* The uncertainties on the JEFF-3.1.2 based cross sections are calculated with the covariance matrices from ENDF/B-VII.1.

Neutron spectrum averaged cross-sections are defined by following equation:

$$\widehat{\sigma} = \frac{\int \sigma(E)\phi(E)dE}{\int \phi(E)dE}.$$

Such cross sections can be calculated with MCNP using the track-length (F4) tally along with the appropriate tally multiplier (FM4) to derive simultaneously the reaction rate (numerator) and neutron flux (denominator). In this way MARK III spectrum averaged cross sections have been calculated for a series of reactions. The results for the most commonly used reactions are summarised in Table 2. Pointwise continuous energy nuclear data from IRDFF-1.02 [5, 6] have been used. For reactions that were not included in IRDFF-1.02, the JEFF-3.1.2 [7] library was adopted.

In order to calculate the uncertainty on the spectrum averaged cross sections, the NJOY99.396 code [8, 9] was selected. The NJOY routine *errorr* [10] is a dedicated tool used to produce multi-group cross-section covariances from covariance data in ENDF-6 [11] format. One-group cross-section uncertainties were then produced through pure nuclear data covariance propagation.

The covariance data were taken from the IRDFF-1.02 files. The lack of covariance information in JEFF-3.1.2 drove our choice to the ENDF/B-VII.1 general purpose library for the uncertainty calculation of these cross sections. The results are summarised in Table 2.

Although MCNP returns the stochastic uncertainty of the spectrum for each energy bin, we omitted this information in the NJOY uncertainty calculation since the code lacks the proper features to

handle it. Thus, we limited ourselves to merely propagating uncertainties and correlations coming from the nuclear data.

The absolute value of the MARK III neutron flux is provided through the calibration factor. This factor is the ratio of the neutron flux in the centre of MARK III (determined via activation dosimetry) to the monitor fission chamber count rate. For this purpose multiple activation dosimeters have been measured. The average value obtained from each reaction is summarised in Table 1. Rather than taking the weighted average, the calibration factor obtained with the Ni dosimeters will be used for the normalisation of the measurements.

Neutron flux gradients are present in the MARK III converter. These have been experimentally determined and correction functions have been obtained via a fit through the experimental data.

The axial variation of the neutron flux was measured with a natural uranium fission chamber and via activation dosimetry with Indium foils. The results obtained with both methods are in excellent agreement.

The radial variation of the neutron flux was determined via activation dosimetry with Indium foils. For this purpose a circular Indium foil was pre-punched into 5 concentric rings.

Finally, in order to correct for possible perturbations induced by the detector or foil itself, a suited model can be made and included in the MCNP input file.

4. Discussion

Throughout the qualification of the MARK III irradiation field, a number of items requiring further investigation have been identified. These are briefly summarised below.

The Mark III spectrum averaged cross sections were not only calculated using the nuclear data library indicated in Table 2. Instead, for the sake of comparing nuclear data libraries, each cross section was calculated using three different libraries: IRDFF-1.02, JEFF-3.1.2 and ENDF/B-VII.1. We observed a good agreement between the results obtained with the different libraries for most reactions. However, in some cases differences exceeding the uncertainties have been observed. This will be further investigated.

We found that the JEFF-3.1.2 library does not contain covariance information for the cross sections. Therefore all uncertainty calculations were performed with the covariance information from the IRDFF-1.02 and ENDF/B-VII.1 nuclear data libraries.

From Table 2 one observes that some of the calculated uncertainties on the cross sections are extremely low. For several reactions uncertainties of $<0.5\%$ have been obtained, which seems unreal even for cross sections that can be determined with absolute measurements. The uncertainties in Table 2 are obtained via error propagation using the covariance data from the IRDFF-1.02 and ENDF/B-VII.1 libraries. A wrong evaluation of the systematic components in the covariance data could for example be the reason for obtaining (too) low uncertainties. This will be further investigated. In general, the issue of too low uncertainties generated by evaluation methods compared to larger uncertainties of experimental data has been observed [12] but not yet satisfactorily solved.

5. Conclusion

The ^{235}U PFNS in the MARK III converter of the BR1 reactor has been qualified. The absolute neutron flux inside MARK III has been determined via activation dosimetry. A full MCNP model of the BR1 reactor and of the MARK III device has been created. Correction factors (or, equivalently, spectrum averaged cross sections) have been calculated to directly relate the slightly perturbed MARK III spectrum to the pure ^{235}U PFNS. The qualification of the neutron flux has been executed following ISO/IEC 17025 standards.

Different nuclear data libraries have been used for this work. We have observed discrepancies for some reactions between different libraries, and in particular potential problems with the covariance data. This will be the subject of future work.

References

[1] V. Gressier, Radiation Protection Dosimetry (2013), doi 10.1093/rpd/nct328

[2] J. Wagemans, E. Malambu, L. Borms, JAI **9**(3), (2012), doi 10.1520/JAI104024

[3] X-5 Monte Carlo Team, MCNP–A General Monte Carlo N-Particle Transport Code, Version 5 – Vol. I-III: Overview and Theory, Los Alamos National Laboratory report LA-UR-03-1987 (April 2003, revised 2/1/2008)

[4] M. B. Chadwick et al., ENDF/B-VII.1 nuclear data for science and technology: Cross sections, covariances, fission product yields and decay data. Nuclear Data Sheets **112**(12):2887-2996, 2011

[5] R. Capote, K. I. Zolotarev, V. G. Pronyaev, and A. Trkov, Journal of ASTM International (JAI)-Vol. **9**, Issue 4, April 2012,JAI104119

[6] E. M. Zsolnay, R. Capote, H. K. Nolthenius, and A. Trkov, Technical report INDC(NDS)-0616, IAEA, Vienna, 2012

[7] A. J. Koning et al., ed., The JEFF-3.1 nuclear data library, JEFF Report 21,NEA No. 6190, OECD (2006)

[8] R. E. MacFarlane and D.W. Muir. The NJOY nuclear data processing system, version 91. Technical Report LA-12740-M, Los Alamos National Laboratory, 1994

[9] R. E. MacFarlane, A.C. Kahler. Methods for Processing ENDF/B-VII with NJOY, Nuclear Data Sheets, Vol. **111**, Issue 12, December 2010, Pages 2739-2890, 2010

[10] CSEWG Document ENDF-102. ENDF-6 Formats Manual Data Formats and Procedures for the Evaluated Nuclear Data Files ENDF/B-VI and ENDF/B-VII. Technical Report BNL-90365-2009 Rev. 1, National Nuclear Data Center, 2010

[11] R. E. MacFarlane and A.C. Kahler. Methods for processing ENDF/B-VII with NJOY. Nuclear Data Sheets **111**:2739-2890, 2010

[12] C. M. Mattoon, P. Obložinský, J. Korean Phys. Soc. **59**,1242, doi: 10.3938/jkps.59.1242